Influence of Blending Sequence on Micro- and Macrostructure of PA6/mEPDM/EPDMgMA Blends Reinforced with Organoclay

R. Gallego,[1] D. García-López,[2] S. López-Quintana,[2] I. Gobernado-Mitre,[2] J. C. Merino,[1,2] J. M. Pastor[1,2]

[1]*Department of Physics of the Condensed Matter, E.T.S.I.I. University of Valladolid, 47011 Valladolid, Spain*
[2]*CIDAUT, Foundation for Research and Development in Transport and Energy. Parque Tecnológico de Boecillo, E-4715 Valladolid, Spain*

Received 28 November 2007; accepted 6 February 2008
DOI 10.1002/app.28141
Published online 21 April 2008 in Wiley InterScience (www.interscience.wiley.com).

ABSTRACT: The structure of the PA6/mEPDM/EPDMgMA/organoclay ternary hybrids was characterized and related to its properties. The nanoblends were prepared through four different blending sequences based on one- or two-step processes: (1) The PA6/organoclay nanocomposite was prepared and then mixed with the mEPDM+ EPDMgMA compound; (2) the mEPDM+EPDMgMA+ organoclay compound was first prepared and then mixed with PA6; (3) the PA6, mEPDM, EPDMgMA, and organoclays were blended in one step; and (4) the PA6/mEPDM/EPDMgMA blend was prepared and then mixed with the organoclay. The microscopic study of the nanoblends showed a relationship between the blending sequence and the dispersion of the organoclay and the rubber. Nevertheless, the mechanical characterization showed slight differences between the blending sequence because of the presence of the organoclay in the matrix, rubber, or interface. © 2008 Wiley Periodicals, Inc. J Appl Polym Sci 109: 1556–1563, 2008

Key words: polyamide nanoblends; maleated EPDM; extruder; blending sequence; tensile properties; notched impact strength

INTRODUCTION

Polyamides are defined as pseudoductile polymers because of their high energy for craze initiation when compared with the so-called brittle matrices. Pseudoductile matrices deform under an uniaxial tensile stress state mainly by shear yielding, whereas crazing is in general the deformation mechanism of brittle matrices. However, polyamides become brittle in the presence of molding flows, environmental abuse, poor design, or, more generally, in the presence of a stress concentrator that limits their industrial application.[1]

Blending is a well-known method for modifying polyamide properties. Most of the research and development works in polyamide-6 are directed to the improvement of properties like impact strength by blending with a properly functionalized elastomeric phase.[2–12] Blends of polyamides and unfunctionalized elastomers have low impact toughness because the rubber particles formed during melt blending are relatively large.[13,14] A compatibilizer, generally the same elastomer functionalized with a reactive group such as maleic anhydride (MA), is used to improve the interfacial adhesion of the PA/elastomer blends.[15,16] Reactive compatibilizers containing maleic anhydride form a chemical linkage through the reaction of anhydride groups with the polyamide-end groups. This reaction causes the graft copolymer which enhances the interfacial compatibility of immiscible polymer blends.[17] Maleic anhydride-*grafted*-ethylene-propylene elastomers, EPR-*g*-MA, are frequently used for toughening polyamides.[3,10,15,18,19] Commercial products like these typically contain $\sim$ 1% by weight of grafted maleic anhydride and give rise to a rubber particle population in nylon 6 matrix that is in a satisfactory size range for toughening.[19]

For the last years, polymeric nanocomposites have attracted a great interest both in industry and academia because of the ability of the clay platelets of intercalating and exfoliating. The addition of clay at low loadings in those materials provokes the improvement in several properties such as mechanical and gas transport properties, fire retardancy, and temperature resistance, among others.[20] This improvement is due to the highest aspect ratio of the

Correspondence to: R. Gallego (raugal@cidaut.es).
Contract grant sponsor: Ministerio de Educación y Ciencia (Program Torres Quevedo); Contract grant number: MAT2005-06627-C03.
Contract grant sponsors: Council of Education of the Castilla and Leon Government and the European Social Fund.

clay platelets and also to the modification of the montmorillonite which plays a principal role in the intercalation and exfoliation into the polymeric matrix.[21]

Nowadays, there is an increasing study on the effect on combining both blends of polymers and nanocomposites, because it is the way of obtaining balanced properties between modulus and impact strength among others. These works are focused on either improving mechanical properties of polymeric blends reinforced with nanoclays,[22–24] or improving impact strength of nanocomposite materials toughened with a proper functionalized elastomer.[25–29]

However, only a few number of papers have been published providing an insight in the preparation of polyamide blends of nanocomposites with different blending sequence. Some of them are based on blends of nylon66/SEBS-*g*-MA/organoclay, showing that the best blending sequence is that one in which the organoclay is blended with the nylon 66 initially, mixing later with SEBS-*g*-MA for maximizing the notched impact strength because the organoclays are present mainly in the thermoplastic phase.[27,30] Wang et al.[31] have studied the influence of different blending sequence and different packing injection molding on blends of PA6/EPDM-*g*-MA/organoclay. They have concluded that the blending sequence has not much influence on the mechanical properties and one-step blending sequence had already satisfied balanced mechanical properties. García-López et al.[32] have investigated the blending sequence of PA6/mEPDM/EPDMgMA/organoclay blends changing the screw speed depending on the component added to the extruder. They concluded that the best balanced thermal, mechanical, and impact properties were achieved when the blend was extruded first, adding the organoclay later. Similar studies have been developed based on different matrix such as PBT[33,34] and PP,[35] which show the effect of the blending sequence in the extrusion process.

In this study, we used a blend of 50/50 of two rubbers, mEPDM and a toughening agent, EPDMgMA, and a polar organoclay as a reinforcing material to obtain balanced toughness and elastic stiffness of polyamide 6. The compatibilizer was used as an interfacial agent for generating the copolymer polyamide 6-*co*-EPDMgMA, which results in a fine and homogenous dispersion of the rubber into the polyamide 6. The aim of this work is the evaluation of the blending sequence in a blend 80/20 of polyamide 6/rubber, to know how the blending sequence affects the microstructure of the blends reinforced with clay and especially the dispersion of the organoclays in the blends using the extruder conditions previously determined.[36] This article deals with the changes in tensile, impact properties, and heat deflection temperature relating to microstructure and blending sequence.

EXPERIMENTAL

Materials and blends preparation

All materials used in this work are supplied for commercial sources. Polyamide 6 was supplied by DSM (Sittard, The Netherlands), commercialized as Akulon F130C. This polyamide 6 has a viscosity number of 195 cm^3/g determined by ISO 307 at temperature of 240°C. The rubber used for toughening the polyamide 6 was an ethylene–propylene–diene metallocene terpolymer, commercialized as Nordel IP3722P supplied by Dupont (Barcelona, Spain) with an ethylene content of 71 wt %. The compatibilizer was the same EPDM grafted with maleic anhydride supplied by Crompton (Geismar, LA) and commercialized as Royaltuf 498, which contains 72.5 wt % of ethylene, 0.95 wt % of ethylenenorbornene, and 1 wt % of grafted maleic anhydride. An antioxidant Irganox B1171 (blend 1 : 1 of Irganox 1098 and Irgafos 168 from Ciba) was employed to diminish the effect of the temperature and compounding conditions in polyamide 6. This antioxidant was used to prepare a polyamide masterbatch, which was added in 0.2 wt % before blend preparation. The montmorillonite (MMT) used in this study was supplied by Süd Chemie with a trade name of Nanofil® 8 (Louisville, KY). The surfactant used in this montmorillonite was diasteryldimethyl-amonium chloride ($M_2(HT)_2$). M and HT represent methyl and tallow-based product in which the majority of the doubled bonds have been hydrogenated. The amount of surfactant is about 45% calculated by means of thermogravimetric analysis (TGA).

Prior to the melting processing step, PA6 and organoclay were dried at 80 and 60°C, respectively, for 24 h in an oven. The nanoblends were prepared in a Leistritz corotating twin-screw extruder (L/D = 27, L = 0.972 mm) at a temperature profile described in Table I. The screw speed was fixed at 145 rpm and the feed rate was 6 kg/h. Four different blending sequences were developed to know the effect on the microstructure and macrostructure of the blends. As shown in Table II, either a single-step or two-step compounding method was employed for the preparation of the nanoblends: (1) NBA: (PA6/MMT + (mEPDM+EPDMgMA)) (75/10/10/5) means PA6/MMT nanocomposite was prepared and then mixed with the mEPDM+EPDMgMA compound in a second step; (2) NBB: (PA6 + (mEPDM/EPDMgMA/MMT)

TABLE I
Experimental Conditions of the Blending Extrusion for Blends

Profile	Feed rate (kg/h)	Temperature profile (°C)									
		T1	T2	T3	T4	T5	T6	T7	T8	T9	Die
A	6	145	200	230	250	250	250	250	240	235	230
B		245					250				

TABLE II
Samples and Blending Sequence

Sample	Feed port 1	Feed port 2	Temperature profile
RB	mEPDM+EPDMgMA	PA6	A
NBA	PA6	OMMT	B
	mEPDM+EPDMgMA	PA6/ OMMT	A
NBB	mEPDM+EPDMgMA	OMMT	A
	mEPDM/EPDMgMA/ OMMT	PA6	
NBC	PA6+mEPDM+EPDMgMA	OMMT	A
NBD	mEPDM+EPDMgMA	PA6	A
	PA6/mEPDM/EPDMgMA	OMMT	

(75/10/10/5) means mEPDM+EPDMgMA+MMT compound was first prepared and then mixed with PA6; (3) NBC: (PA6+mEPDM+EPDMgMA+MMT) (75/10/10/5) means PA6, mEPDM, EPDMgMA, and MMT were blended in one step; and (4) NBD: (PA6/mEPDM/EPDMgMA + MMT) (75/10/10/5) means PA6/mEPDM/EPDMgMA blend was prepared and then mixed with the MMT.

The nanoblends obtained were injection-molded into test pieces by using an injection molding machine (Margarite JSW110) after being dried at 80°C for 24 h. The temperature of the cylinders was 230–250°C and the mold temperature was 80°C.

TGA was used to determine the clay content in the obtained nanocomposites. Thermograms were obtained in nitrogen atmosphere with a heating rate of 10°C/min using a Mettler Toledo TGA851. The montmorillonite content, not the amount of organoclay, because the silicate is the reinforcing component, was measured by TGA, being around 5 wt % for all the nanocomposites.

Mechanical testing

The Notched Izod test were performed at temperatures of 25 and −30°C on a Ceast Resil Impactor according to the ISO 180 : 2000 standard equipped with a thermal chamber. The average values were calculated from seven runs for each sample. Tensile properties were measured according to UNE-EN ISO 527-1 and 527-2 with an Instron Model 5500R6025. Modulus was determined at a crosshead rate of 1 mm/min, while tensile strength and elongation at break were collected at 10 mm/min.

Heat deflection temperature (HDT) was determined in an HDT-VICAT tester microprocessor (CEAST 6911.000) according to UNE-EN ISO 75-1 and using a load of 1.8 MPa.

Small-angle X-ray scattering

X-ray diffraction of the OMMT and the nanoblends were performed in a Philips X'Pert MPD using Cu Kα radiation to evaluate the evolution of the clay d_{001} reflection. The samples were taken from the middle of the tensile bar.

Transmission electron microscopy

To investigate the dispersion of the organoclay layers in the nanoblends, ultrathin sections ranging from 30 to 50 nm in thickness were cryogenically cut with a diamond knife from the central part of the injection-molded bars, perpendicular to the flow direction in liquid nitrogen environment at −50°C using a RMC PowerTome XL microtome. Sections were collected on a 300-mesh cooper transmission electron microscopy (TEM) grid and subsequently dried with filter paper. The specimens were examined using a JEOL 2010 TEM with LaB_6 filament operating at an accelerating voltage of 120 kV. Specimens for observing rubber particles were stained with 2% aqueous solution of phosphotungstic acid for 40 min.

Scanning electron microscopy

A Jeol-820 scanning electron microscope (SEM) was used to research the rubber particle size and particle size distribution. The injection-molded specimens were broken cryogenically in liquid nitrogen and the elastomeric phase was extracted from the surface by etching with boiling xylene during at least 6 h. After sputter coating with a thin film of gold, the specimens were examined. An accelerating voltage of 20 kV and a magnification range from 1300× to 10,000× was used.

RESULTS AND DISCUSSION

Effect of blending sequence on the microstructure of the nanoblends

Figures 1–3 show the small-angle X-ray scattering (SAXS), TEM, and SEM results, respectively, to com-

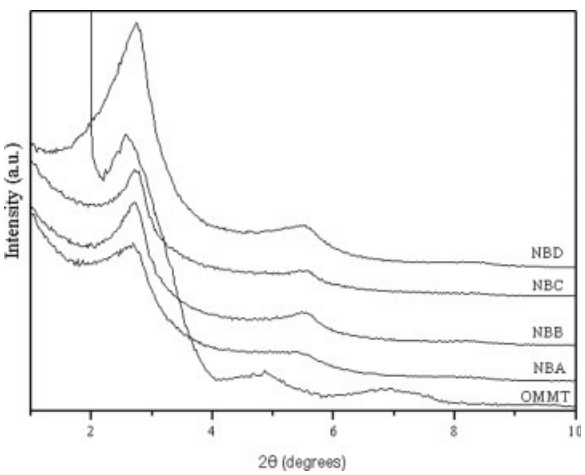

Figure 1 X-ray diffraction patterns of organo-montmorillonite (OMMT) and its blends.

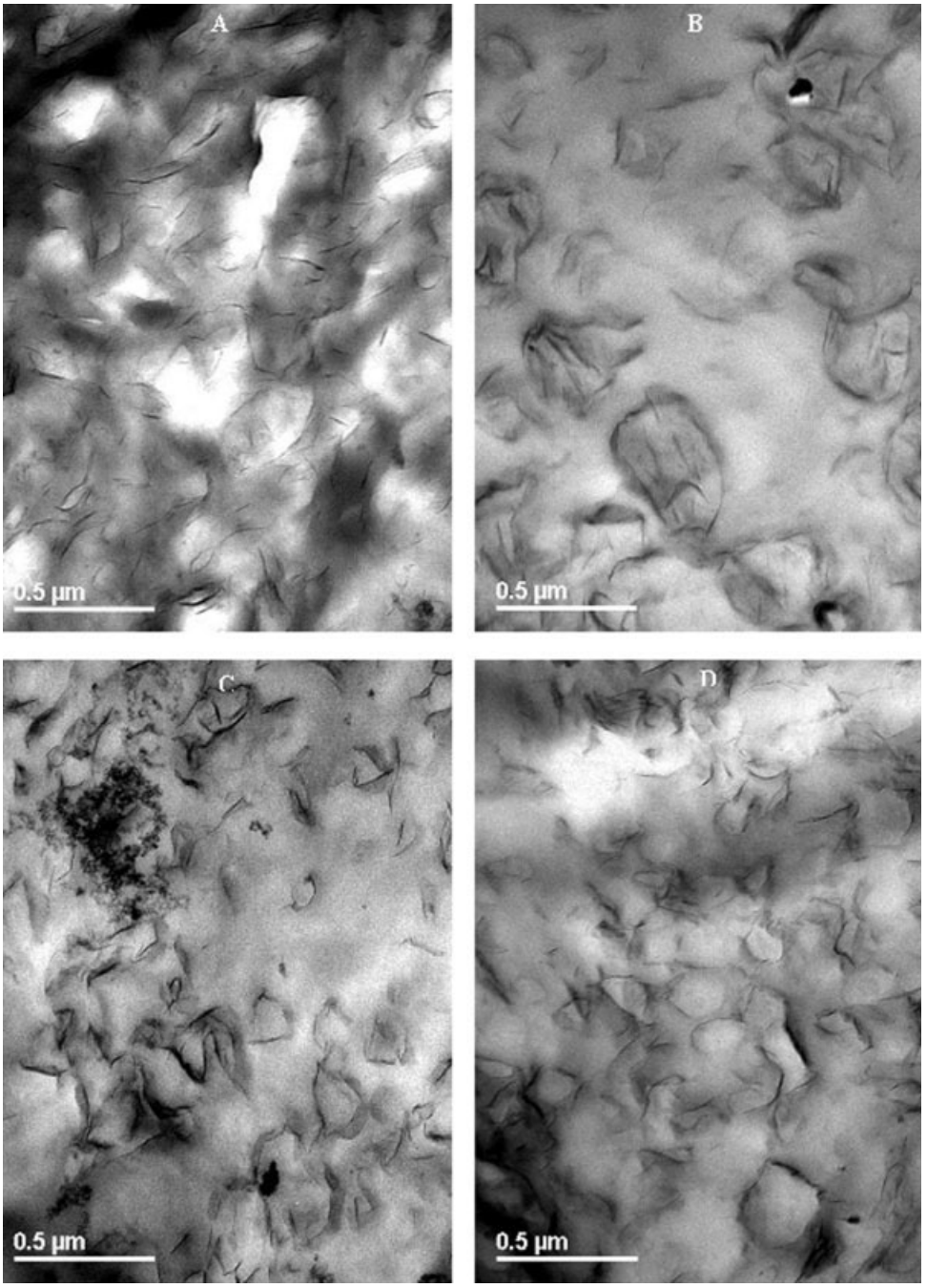

Figure 2 TEM photomicrographs of blends reinforced with OMMT (A) NBA; (B) NBB; (C) NBC; and (D) NBD.

pare the effect of blending sequence on the microstructure of the polymer blends. X-ray results show the diffraction peak at a 3.3 nm which is the same distance of the pristine organoclay. Although all the blends show this characteristic peak, there are some differences between the blending sequences.

The NBA blend was made in two steps, first the OMMT was placed selectively on the polyamide 6, presenting a weaker peak than the others. This behavior is due to the ability of the polyamide 6 of interacting with the OMMT. The TEM photomicrographs presented in Figure 2(A) for this blend corroborate the SAXS results. In this photomicrograph, the presence of some platelets completely exfoliated in the polyamide 6 can be observed, showing at the same time some particles composed by several platelets. There is also an amount of OMMT present in the interface between the matrix and the dispersed phase. This behavior is due to the blending sequence in which, in the first step the organoclay is added at the same time with the polyamide 6 causing the interaction between the surfactant in the OMMT

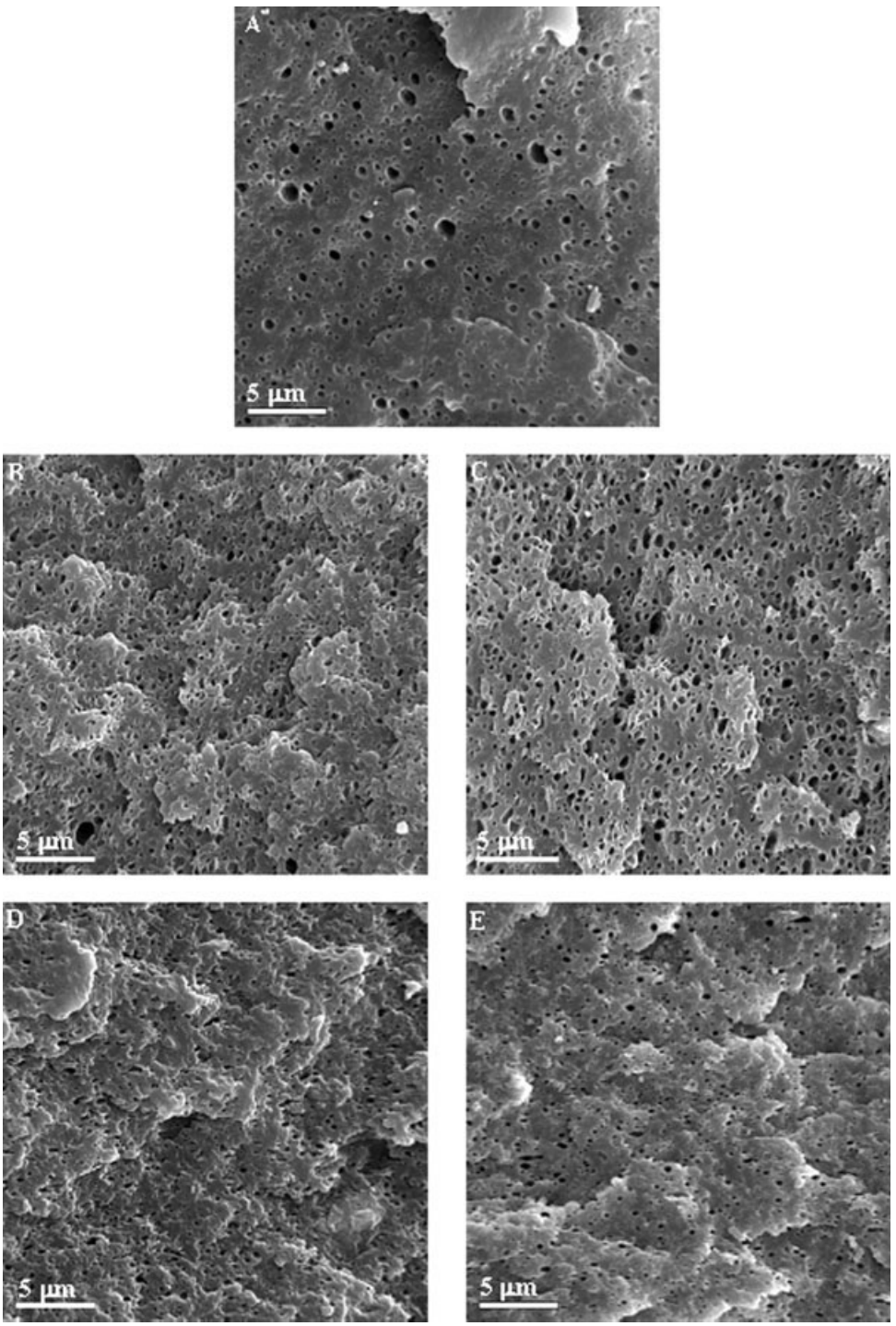

Figure 3 SEM photomicrographs of the reference blend and blends reinforced with OMMT (A) RB; (B) NBA; (C) NBB; (D) NBC; and (E) NBD.

with the end amine group present in the polyamide 6. In the second step, the rubber is added, then, the OMMT would be attracted by the maleic anhydride groups of the compatibilizer. Nevertheless, it might cause an interaction between the matrix and the surfactant which prevents the entering of the organoclay into the rubber, which in turn causes the presence of some particles of organoclay in the interface between the matrix and the dispersed phase. However, it should be noticed here that most of the organoclay appears on the polyamide matrix. The morphology of the dispersed phase is presented in Figure 3(B). As it can be seen, the rubber particles are homogenously dispersed into the matrix.

On the other hand, the NBB blend shows an opposite behavior when compared with the NBA blend.

TABLE III
Characterization of PA6/mEPDM/EPDMgMA Blend (RB) and PA6/mEPDM/ EPDMgMA/MMT Nanoblends (NBA, NBB, NBC, and NBD)

		RB	NBA	NBB	NBC	NBD
E (MPa)		1439 ± 4	2900 ± 23	2820 ± 39	2870 ± 11	2777 ± 44
σ_y (MPa)		38.7 ± 0.1	47.9 ± 0.5	48.2 ± 1.8	47.7 ± 0.2	49.3 ± 0.4
ε_b (%)		221.4 ± 12	60.4 ± 14.3	42.8 ± 4.6	8.3 ± 1.4	10.3 ± 3.5
HDT (°C)		49.9 ± 0.3	81.3 ± 2.2	80.6 ± 3.9	88.9 ± 3.9	88.4 ± 2.0
I_s (kJ/m^2)	25°C	49.6 ± 1.2	12.6 ± 0.5	15.1 ± 0.6	11.2 ± 0.6	14.5 ± 3.1
	−30°C	15.2 ± 0.5	3.3 ± 0.4	3.7 ± 0.3	5.3 ± 0.5	6.6 ± 0.4

In this blend, the rubber and the OMMT was added to the extruder and in the second step, the polyamide 6 was added. Figure 2(B) shows that most of the organoclay appears in the rubber. However, the low polar nature of the rubber cannot exfoliate the silicate layers resulting in an intercalated structure in the rubber phase. Furthermore, there are some particles in the interface between the matrix and the rubber because of the higher polarity of the interactions between the maleic anhydride groups of the compatibilizer and the end amine groups of the polyamide 6. Additionally, in this blend, the rubber particle size [Fig. 3(C)] is larger than in the others due to a lower compatibilization which in turns diminishes the interaction between both polyamide 6 and rubber. The organoclay behavior could be corroborated by the SAXS results presented in Figure 1. In this pattern, the basal diffraction peak of the pristine organoclay can also be seen. This peak is broader than that observed in NBA due to the higher intercalation observed when compared with the other blend.

As described in the NBB blend, here the X-ray patterns (Fig. 1) show a broader peak for the NBC and NBD blends. This behavior has been corroborated with TEM photomicrographs presented in Figure 2(C,D) for NBC and NBD, respectively. As it can be seen, there are some isolated platelets in the matrix, but also there are some intercalated structures in the interface between both phases of the blends. Although these blends have been produced in a different blending sequence, i.e., NBC was compounded in one step, while NBD was compounded in two steps, the organoclay shows the same behavior. In the NBC blend, all the components of the blends were added at the same time into the extruder machine, then, the major polarity of the polyamide 6 causes the attachment of the OMMT into the matrix. However, the linkage between the rubber and the polyamide 6 through the creation of the PA6-*g*-EPDM copolymer has also a high polarity which brings the OMMT into the interface as well as into the matrix. Finally, the two polymers are first blended and then the OMMT was added to produce the NBD blend. This blending sequence causes the same behavior to the one achieved in NBC blend due to the same reasons explained earlier. The rubber particle size distribution of NBC and NBD blends [Fig. 3(D,E), respectively] are similar and smaller than the ones observed in the other blends due to the presence of the OMMT that increases the viscosity of the matrix, and therefore leads to an increased mastication and deformation of the dispersed polymeric phase.

Mechanical characterization of the nanoblends

Table III shows the results of the mechanical characterization of the reference blend and its nanoblends. In all the nanoblends, a higher value of all the properties related to the stiffness was achieved when compared with the reference blend (RB). Nevertheless, in properties such as impact strength a decrease was obtained when compared with RB. These results agree with our previous reported results.[32]

The parameters affecting the compounding process of these nanoblends are the same and the only difference among them is the incorporation of the materials into the extruder. Therefore, the presence of the organoclay in the different parts of the blends will provoke the differences among the mechanical properties.

In NBA blend, most of the organoclay is intercalated-exfoliated into the PA6 matrix as it was observed by means of TEM. This behavior provokes the highest value of the Young modulus (E) when compared with the rest of the nanoblends. NBC and NBD present some particles of clay in the matrix, but a high exfoliation leading to lower values of the Young modulus was not achieved. For the NBB blend, a higher value of Young's modulus than expected was achieved due to the presence of the organoclay into the rubber, as observed by TEM which provoked the stiffness of the rubber component.

In NBC and NBD [Figs. 2(C,D) and 3(D,E)], the rubber is surrounded by stacks of clay platelets as observed by means of TEM and SEM. This behavior was obtained by the compounding process because NBC was extruded in one step and NBD in two steps. The attraction of the maleic anhydride groups

by the polyamide 6 is high but also the interface has a high polarity, leading to the attraction of the organoclay as well as to the matrix. Kelnar et al.[37] have obtained the highest toughness in the nanoblends with this kind of structure because of a compatibilization effect and favorable ''core-shell'' structure induced by the clays. In our samples, the same effect was observed mainly in the NBD blend and consequently the highest impact strength (I_s) at low temperature was achieved.

The higher the presence of organoclay in the interface, the lower is the elasticity of the nanoblends as it is shown by the values of the elongation at break. On the other hand, the presence of the organoclay in the interface provokes higher values of the HDT due to the higher stiffness of the interface.

Commonly, the yield strength (σ_y) shows, among others, the interaction between the polymer and the filler.[38] As Table III shows, the interaction between the filler and the polymer should be higher, because the values of yield strength are greater than that obtained in the reference blend. Therefore, it is reasonable that the highest value of yield strength was achieved in NBD blend due to the highest content of OMMT in the interface.

Our goal in this work was the evaluation of the blending sequence and how it affects the mechanical properties. In this way, the best balanced mechanical properties were achieved in NBA and NBD blends, in which the nanoblends were developed in two steps. Although in both the blending sequences good balanced mechanical properties were achieved, the dispersion of the organoclay in the matrix will be the most appropriate sequence due to an easier control of the exfoliation which will lead to a higher stiffness without a very important lost in the toughness.

CONCLUSIONS

The blending sequence shows a high influence on the dispersion of the organoclay and the rubber. Although there is not much influence on the modulus, the achieved microstructure has produced some differences on the other mechanical properties. The presence of the organoclay in the matrix or in the interface between both phases is the best way to achieve equilibrium between stiffness and toughness. Nevertheless, the presence of the organoclay in the interface has provoked the reduction of the elongation at break values, while the HDT property has increased its value because of the stiffness caused by the platelets of MMT. On the other hand, blending the organoclay with the rubber component is detrimental to achieve good balanced mechanical properties.

The best balance between stiffness and toughness is obtained by blending first the organoclay with the polyamide 6 and then, blending this nanocomposite with the elastomeric component. However, the presence of the organoclay in the interface has improved the notched impact strength due to the compatibilization effect provoked by the organoclay.

Even though we have obtained a good balance between stiffness and toughness in the preferred blending sequence, further studies are being developed to improve the toughness, without an important loss in stiffness, changing the amount of clay and compatibilizer with the preferred blending sequence achieved in this work.

The authors thank Prof. Donald R. Paul from the Department of Chemical Engineering and Texas Materials Institute, University of Texas at Austin, for providing the TEM facilities.

References

1. Burgisi, G.; Paternoster, M.; Peduto, N.; Saraceno, A. J Appl Polym Sci 1997, 66, 777.
2. Cimmino, S.; Coppola, F.; D'Orazio, L.; Greco, R.; Maglio, G.; Malinconico, M.; Mancarella, C.; Martuscelli, E.; Ragosta, G. Polymer 1986, 27, 1874.
3. Oshinski, A. J.; Keskkula, H.; Paul, D. R. Polymer 1996, 37, 4891.
4. Horiuchi, S.; Matchariyakult, N.; Yase, K.; Kitano, T.; Choi, H. K.; Lee, Y. M. Polymer 1996, 37, 3065.
5. Horiuchi, S.; Matchariyakult, N.; Yase, K.; Kitano, T.; Choi, H. K.; Lee, Y. M. Polymer 1997, 38, 59.
6. Orderkerk, J.; Groeninckx, G. Polymer 2002, 43, 2219.
7. Wilkinson, A. N.; Clemens, M. L.; Harding, V. M. Polymer 2004, 45, 5239.
8. Huang, J. J.; Keskkula, H.; Paul, D. R. Polymer 2004, 45, 4203.
9. Wang, C.; Su, J. X.; Li, J.; Yang, H.; Zhang, Q.; Du, R. N.; Fu, Q. Polymer 2006, 47, 3197.
10. Huang, J. J.; Keskkula, H.; Paul, D. R. Polymer 2006, 47, 639.
11. Horiuchi, S.; Matchariyakult, N.; Yase, K.; Kitano, T.; Choi, H. K.; Lee, M. Polymer 1997, 38, 6326.
12. González-Montiel, A.; Keskkula, H.; Paul, D. R. Polymer 1995, 36, 4587.
13. Thomas, S.; Groeninckx, G. J Appl Polym Sci 1998, 71, 1405.
14. Thomas, S.; Groeninckx, G. Polymer 1999, 40, 5799.
15. Huang, J. J.; Keskkula, H.; Paul, D. R. Polymer 2006, 47, 624.
16. Yu, Z. Z.; Ou, Y. C.; Hu, G. H. J Appl Polym Sci 1998, 69, 1711.
17. Tjong, S. C.; Ke, Y. C. Eur Polym J 1998, 34, 1565.
18. Okada, O.; Keskkula, H.; Paul, D. R. Polymer 2001, 42, 8715.
19. Okada, O.; Keskkula, H.; Paul, D. R. Polymer 2000, 41, 8061.
20. Utraki, L. A. In Clay-Containing Polymeric Nanocomposites; Utracki, L. A., Ed.; Rapra Technology, United Kingdom, 2004; p 1.
21. Ray, S. S.; Okamoto, M. Prog Polym Sci 2003, 28, 1539.
22. Khatua, B. B.; Lee, D. J.; Kim, Y. H.; Kim, J. K. Macromolecules 2004, 37, 2454.
23. Yoo, Y.; Park, C.; Lee, S.; Choi, K.; Kim, D. S.; Lee, J. H. Macromol Chem Phys 2005, 206, 878.
24. Chow, W. S.; Mosd Ishak, Z. A.; Karger-Kocsis, J.; Apostolov, A. A.; Ishiaku, U. S. Polymer 2003, 44, 7427.
25. Tjong, S. C.; Bao, S. P. J Polym Sci Part B: Polym Phys 2005, 43, 585.
26. González, I.; Eguiazabal, J. I.; Nazabal, J. J Polym Sci Part B: Polym Phys 2005, 43, 3611.

27. Dasari, A.; Yu, Z.-Z.; Mai, Y.-M. Polymer 2005, 46, 5986.
28. Chiu, G.-C.; Lai, S.-M.; Chen, Y.-L.; Lee, T.-H. Polymer 2005, 46, 11600.
29. Ahn, Y.-C.; Paul, D. R. Polymer 2006, 47, 2830.
30. Dasari, A.; Yu, Z.-Z.; Yang, M.; Zhang, Q.-X.; Xie, X.-L.; Mai, Y.-W. Comput Sci Technol 2006, 66, 3097.
31. Wang, K.; Wang, C.; Li, J.; Su, J.; Zhang, Q.; Du, R.; Fu, Q. Polymer 2007, 48, 2144.
32. García-López, D.; López-Quintana, S.; Gobernado-Mitre, I.; Merino, J. C.; Pastor, J. M. Polym Eng Sci 2007, 47, 1033.
33. Park, H.-M.; Lee, J.-O.; Ha, C.-S. Polym Eng Sci 2002, 42, 2156.
34. Wu, D.; Zhou, C.; Yu, W.; Xie, F. J Appl Polym Sci 2006, 99, 340.
35. Treece, M. A.; Zhang, W.; Moffitt, R. D.; Oberhauser, J. P. Polym Eng Sci 2007, 47, 898.
36. Gallego, R.; García-López, D.; López-Quintana, S.; Gobernado-Mitre, I.; Merino, J. C.; Pastor, J. M. Polym Bull 2008, to appear.
37. Kelnar, I.; Khunová, V.; Kotek, J.; Kaprálkova, L. Polymer 2007, 48, 5332.
38. Kim, D. H.; Fasulo, P. D.; Rodgers, W. R.; Paul, D. R. Polymer 2007, 48, 5308.